



HAL
open science

Origins and discrimination between local and regional atmospheric pollution in Haiphong (Vietnam), based on metal(loid) concentrations and lead isotopic ratios in PM10

Sandrine Chifflet, David Amouroux, Sylvain Bérail, Julien Barre, Thuoc Chu Van, Oriol Baltrons, Justine Brune, Aurélie Dufour, Benjamin Guinot, Xavier Mari

► To cite this version:

Sandrine Chifflet, David Amouroux, Sylvain Bérail, Julien Barre, Thuoc Chu Van, et al.. Origins and discrimination between local and regional atmospheric pollution in Haiphong (Vietnam), based on metal(loid) concentrations and lead isotopic ratios in PM10. *Environmental Science and Pollution Research*, 2018, 25 (26), pp.26653-26668. 10.1007/s11356-018-2722-7. hal-01862504

HAL Id: hal-01862504

<https://hal.science/hal-01862504>

Submitted on 21 Mar 2019

HAL is a multi-disciplinary open access archive for the deposit and dissemination of scientific research documents, whether they are published or not. The documents may come from teaching and research institutions in France or abroad, or from public or private research centers.

L'archive ouverte pluridisciplinaire **HAL**, est destinée au dépôt et à la diffusion de documents scientifiques de niveau recherche, publiés ou non, émanant des établissements d'enseignement et de recherche français ou étrangers, des laboratoires publics ou privés.



Origins and discrimination between local and regional atmospheric pollution in Haiphong (Vietnam), based on metal(loid) concentrations and lead isotopic ratios in PM₁₀

Sandrine Chifflet¹ · David Amouroux² · Sylvain Bérail² · Julien Barre² · Thuoc Chu Van³ · Oriol Baltrons² · Justine Brune⁴ · Aurélie Dufour¹ · Benjamin Guinot⁵ · Xavier Mari¹

Received: 24 October 2017 / Accepted: 5 July 2018
© Springer-Verlag GmbH Germany, part of Springer Nature 2018

Abstract

Southeast Asia is a hotspot of anthropogenic emissions where episodes of recurrent and prolonged atmospheric pollution can lead to the formation of large haze events, giving rise to wide plumes which spread over adjacent oceans and neighbouring countries. Trace metal concentrations and Pb isotopic ratios in atmospheric particulate matter < 10 μm (PM₁₀) were used to track the origins and the transport pathways of atmospheric pollutants. This approach was used for fortnightly PM₁₀ collections over a complete annual cycle in Haiphong, northern Vietnam. Distinct seasonal patterns were observed for the trace metal concentration in PM₁₀, with a maximum during the Northeast (NE) monsoon and a minimum during the Southeast (SE) monsoon. Some elements (As, Cd, Mn) were found in excess according to the World Health Organization guidelines. Coal combustion was highlighted with enrichment factors of As, Cd, Se, and Sb, but these inputs were outdistanced by other anthropogenic activities. V/Ni and Cu/Sb ratios were found to be markers of oil combustion, while Pb/Cd and Zn/Pb ratios were found to be markers of industrial activities. Pb isotopic composition in PM₁₀ revealed an important contribution of soil dusts (45–60%). In PM₁₀, the Pb fraction due to oil combustion was correlated with dominant airflow pathways (31% during the north-easterlies and 20% during the south-easterlies), and the Pb fraction resulting from industrial emissions was stable (around 28%) throughout the year. During the SE monsoon, Pb inputs were mainly attributed to resuspension of local soil dusts (about 90%), and during the NE monsoon, the increase of Pb in PM₁₀ was due to the mixing of local and regional inputs.

Keywords Airpollution · Haiphong · Enrichment factors · Chemical balances · Lead isotopes · Anthropogenic sources · Local and regional inputs

Responsible editor: Philippe Garrigues

Electronic supplementary material The online version of this article (<https://doi.org/10.1007/s11356-018-2722-7>) contains supplementary material, which is available to authorized users.

✉ Sandrine Chifflet
sandrine.chifflet@mio.osupytheas.fr

¹ CNRS, IRD, MIO UM110, Aix Marseille Université, Université de Toulon, 13288 Marseille, France

² CNRS/UNIV PAU & PAYS ADOUR, Institut des sciences analytiques et de physico-chimie pour l'environnement et les matériaux, UMR5264, 64000 Pau, France

³ Institute of Marine Environment and Resources, Vietnam Academy of Science and Technology (VAST), Danang, Haiphong 246, Vietnam

⁴ IRD, UMR 5119 ECOSYM, Université Montpellier II, Montpellier, France

⁵ Laboratoire d'Aérogologie, Université de Toulouse, CNRS, UPS, 14 avenue Edouard-Belin, 31400 Toulouse, France

Introduction

Atmospheric particulate matter (PM) is a complex mixture of various substances (e.g. organic and elemental carbon, SO₄²⁻, NH₄⁺, trace metals) that may carry signatures of its origins (Duce et al., 1975; Patterson and Settle, 1987; Nriagu and Pacyna, 1988). PM occurs along a size continuum that is operationally defined as: coarse particles (PM₁₀, aerodynamic diameter < 10 μm) emitted from natural and anthropogenic sources, fine particles (PM_{2.5}) mainly produced from anthropogenic activities, and ultrafine particles (PM_{0.1}) derived from PM₁₀ and PM_{2.5} transformations (Cohen et al., 2010a, 2010b; Kim et al. 2012).

Nowadays, anthropogenic PM emissions generally exceed crustal derived sources for trace metals owing to the rapid expansion of industrial activities, motorization, and urbanisation processes (Chen et al., 2005; Chen and Zhang, 2010).

Southeast Asia is one of the most economically dynamic regions in the world. This results in a high production of anthropogenic PM during the combustion of fossil fuels (coal, oil, and natural gas) used for energy production in the residential, commercial and industrial sectors, and for transportation (Duan et al., 2003; Sun et al., 2004; Feng et al., 2005; Wang et al., 2005, 2006a; Okuda et al., 2008). Vietnam has the second largest coal reserves in the region, with 3100 Mt of hard coal and 200 Mt of brown coal at the end of 2011 (BGR, 2013). The majority of these reserves are located in northern Vietnam. The oil produced by the wells located in southeast Vietnam is mainly aimed at the domestic market, with a production of 450 thousand barrels per day. Gas production is exploited offshore southern Vietnam and has grown steadily in the past decade, reaching $9 \times 10^9 \text{ m}^3$ in 2011 (IEA, 2015).

The occurring of large haze events principally made up of anthropogenic PM causes multiple detrimental effects caused by the deterioration of air quality in the region (Ramanathan et al., 2005; R uckerl et al., 2011). In the Asian region, PM composition varies widely in accordance with anthropogenic emissions, as well as natural inputs influenced by the Asian monsoon, which transports desert dust over thousands of kilometres (Cohen et al., 2010b). Trace metal ratios are widely used to infer the origin of PM from their specific chemical composition, by comparing this “fingerprint” with those of potential sources (Nriagu and Pacyna, 1988; Veron et al., 1992; Wedepohl, 1995; Hu et al., 2003). The isotopic composition of an element occurring in PM offers another means of tracking sources of heavy metals and pathways of atmospheric pollution. Although the non-radiogenic lead isotopic composition (^{206}Pb , ^{207}Pb , and ^{208}Pb) is preserved after being naturally transferred in the environment via weathering processes (Murozumi et al., 1969; Doe, 1970; Cumming and Richards, 1975; Stacey and Kramers, 1975; Bollhofer and Rosman, 2000), this composition can vary after mixing with secondary lead sources via industrial processes (Mukai et al., 1991; Wang et al., 2000; Mukai et al., 2001; Zheng et al., 2004; Kom arek et al., 2008).

In many developing countries, monitoring of air pollution is still rare. The few studies conducted in the two main Vietnamese cities, Hanoi and Ho Chi Minh City, have showed the impact of monsoon conditions air quality (Hien et al., 2001, 2002, 2004; Cohen et al., 2010a, 2010b; Hai and Kim Oanh, 2013). To quantify and characterise the origin of atmospheric particles, the authors have used positive matrix factorisation (PMF) to circumvent the lack of specific source fingerprints. This statistical model requires a large number of samples, and the chemical composition of emission sources was based on comparison with profiles of North American sources (Henry et al., 1984, Paatero and Tapper, 1994). Other studies have used the HYPPLIT model to identify the

origin of PM in a rural site in northern Vietnam (Hoang et al., 2014; Gatari et al., 2006). However, information concerning trace metal emissions in Vietnam is still scarce, and chemical compositions of anthropogenic sources from Vietnam have yet to be determined. For the first time, the present year-round monitoring study reports a quantitative measurement of 22 metal(loid)s (Al, As, Cd, Co, Cr, Cu, Fe, Hg, K, Mg, Mn, Na, Nd, Ni, Pb, Rb, Sb, Se, Sr, Ti, V, and Zn) present in PM_{10} collected in Haiphong. In order to better understand the impact of monsoon conditions on air quality in the city, we provide an inventory of lead isotopic compositions (^{204}Pb , ^{206}Pb , ^{207}Pb , and ^{208}Pb) in PM_{10} . To partly fill the knowledge gap, this paper presents characterisations of major emission sources and their relative contributions in Haiphong by discriminating long-range and local inputs. In the present study, we are mainly interested in global atmospheric contamination rather than studying specific extreme events.

Methodology

Study site and PM_{10} sampling

The sampling station is located in Haiphong at about 100 km southeast of Hanoi. With about two million inhabitants, Haiphong is the third largest city in Vietnam and is the main seaport in northern Vietnam. This area is influenced by a subtropical climate with a seasonal differentiation due to the northeast monsoon, which is associated with a dry (cooler) season from November to April and the southeast monsoon itself associated with a wet (warmer) season from May to October (Vu, 1994).

PM_{10} were collected on the roof of the Institute of Marine Environment and Resources (IMER, Haiphong) using a Staplex PM_{10} High Volume Air sampler. The annual survey was conducted from October 2012 to October 2013. Samples were collected every 2 weeks for two consecutive 12-h periods, using quartz fibre filters (Staplex Type TFAQ810 of $20 \times 25 \text{ cm}$). A total of 56 filters were used during the sampling period. The average air volume filtered—calculated using the recorded air flow and the sampling time—was $1147 \pm 126 \text{ m}^3 \text{ filter}^{-1}$. The quartz filters were stored in plastic bags and frozen until analysis. Field blanks were handled identically to the PM_{10} sampling, but were run on the Staplex sampler for only 1 min (Pekney and Davidson, 2005).

Over the course of the sampling period, the wind speed and wind direction data were recorded continuously using an anemometer (Vantage Pro 2, Davis) installed on the roof of the Institute of Marine Environment and Resources.

Analytical procedures

Determination of trace metals in PM₁₀ was conducted following the Standard Operating Procedure in the US Environmental Protection Agency (Method IO-3.5, EPA, 1999). All samples were processed and analysed in a trace metal clean HEPA filtered laboratory (ISO 7), using high purity acids (Fisher, Optima grade) and milliQ water. PFA beakers were cleaned in HNO₃ (10%), sonicated for 2 h, rinsed, and dried in a laminar flow cabinet (class 10). Samples were leached with 10 mL of a pure acids mixture (HF/HCl/HNO₃, 1:6:2), sonicated for 2 h, and heated on a hot-block (100 °C, 4 h). The solutions thus obtained were cooled and diluted in 10 mL of HNO₃ (2%) before analysis. Some elements (Al, Fe, K, Mn, Mg, Na, Se, and V) were analysed with an inductively coupled plasma optical spectrometer (ICP-OES, Perkin Elmer, Optima 8000DV) using an ICP multi-elemental commercial solution (Merck, Certipur) to control the performance of external calibration. Other elements (As, Cd, Co, Cr, Cu, Nd, Ni, Pb, Rb, Sb, Sr, Ti, Zn) were measured by inductively coupled plasma mass spectrometry (Q-ICP-MS, Perkin Elmer, NexION 300X) using Sc and In as internal standards to correct for instrumental mass bias. The digestion procedure was assessed using a certified material for marine sediments (IAEA 433) and a certified material for atmospheric PM (NIOH, SRM B3). All elements were within the satisfactory target recovery of 100 ± 15%, except for Cd (134%). Trace metal concentrations in blank filters were less than 1% of the average trace metal concentrations measured in PM₁₀ samples. Precision and accuracy of analysis were checked with a certified reference material (NIST 1643e). The analytical detection limits were well below the analysed samples. More detailed are presented in Table S1 as Supplementary information.

Lead isotopic analyses (²⁰⁴Pb, ²⁰⁶Pb, ²⁰⁷Pb, ²⁰⁸Pb) were performed with a multi-collector inductively coupled plasma mass spectrometer (MC-ICP-MS, Nu Instruments, Nu Plasma) at a concentration of 200 ppb (Ortega et al. 2012). In order to minimise matrix effects during analysis, lead was extracted and purified by an ion exchange resin (Dowex 1X8, 100–200 mesh, Acros Organics) according to a conventional protocol (Manhès et al., 1978; Monna et al., 1997). An internal isotopic standard of Tl (NIST 997) was added to all samples to correct the instrumental drift. In addition, a standard bracketing method was applied to correct fractionation effects using isotopic standard of Pb (NIST 981). The combination of Tl normalisation and classical bracketing method provided an analytical precision (‰) of 0.0033, 0.0007, and 0.0004 for ^{208/206}Pb, ^{207/206}Pb, and ^{206/204}Pb, respectively.

An AMA 254 mercury analyser (Leco, USA) was used for the determination of total Hg concentration by direct analysis of samples with an AS 254 autosampler. The method does not require any special preparation of samples (Wiśniewska et al.,

2017). Analytical uncertainties were evaluated by measurements of the certified reference material BCR 482 with a recovery of 83.5% and a detection limit of 0.005 µg g⁻¹.

Trajectory cluster analysis

Weather in Haiphong is under the influence of the Asian monsoon, itself characterised by a marked change of wind direction. After meteorological analysis, we classified seasonality during dry (cooler temperature, lower rainfall), transition, and wet (higher temperature, higher rainfall) periods. In order to characterise transport of pollutants, isentropic trajectories extending 48 h backwards at the site were calculated at three different altitudes (500, 1000, and 1500 m) using the NOAA HYSPLIT-4 model (Draxler and Rolph, 2003). However, the accuracy of an individual trajectory is limited by various uncertainties, leading to coarse approximation of air mass origin (Draxler et al., 1999). Large numbers of trajectories were statistically used to identify homogeneous groups of transport pathways. The air trajectories arriving at the site were computed throughout the sampling period from October 2012 to October 2013. For each day, four 6-hourly trajectories with ending times of 00:00, 06:00, 12:00, and 18:00 GMT were calculated, and the data set was split according to seasonality (dry, transitional, and wet periods). Cluster analysis was applied separately to each of the three periods. A detailed description of the clustering process can be found in the NOAA HYSPLIT-4 user's guide.

Cluster analysis showed differing air mass back trajectories according to seasonal differentiation (Fig. 1, Table S2). Due to regional emission zones, the area surrounding Haiphong was classified in three sectors: the northeast (NE) pathway over China; the southeast (SE) pathway over the South China Sea and southern Vietnam; and the southwest (SW) pathway over northern Vietnam, Laos, and Thailand. Clustering results presented a dominant airflow (81%) from the NE sector in the dry season, which decreased in the transitional period (65%). The mean direction of the north-easterly flow moved further south in the wet season. Clustering presented different airflow pathways: 45% from NE, 32% from SE, and 23% from SW. To provide a more precise view of atmospheric pollution in Haiphong, our results are presented and discussed using the NE or SE dominant airflow pathways rather than seasonal differentiation.

Results and discussion

Chemical composition of PM₁₀ and comparison with the literature

Variations of elemental PM₁₀ levels measured in Haiphong according to the dominant airflow pathway are presented in

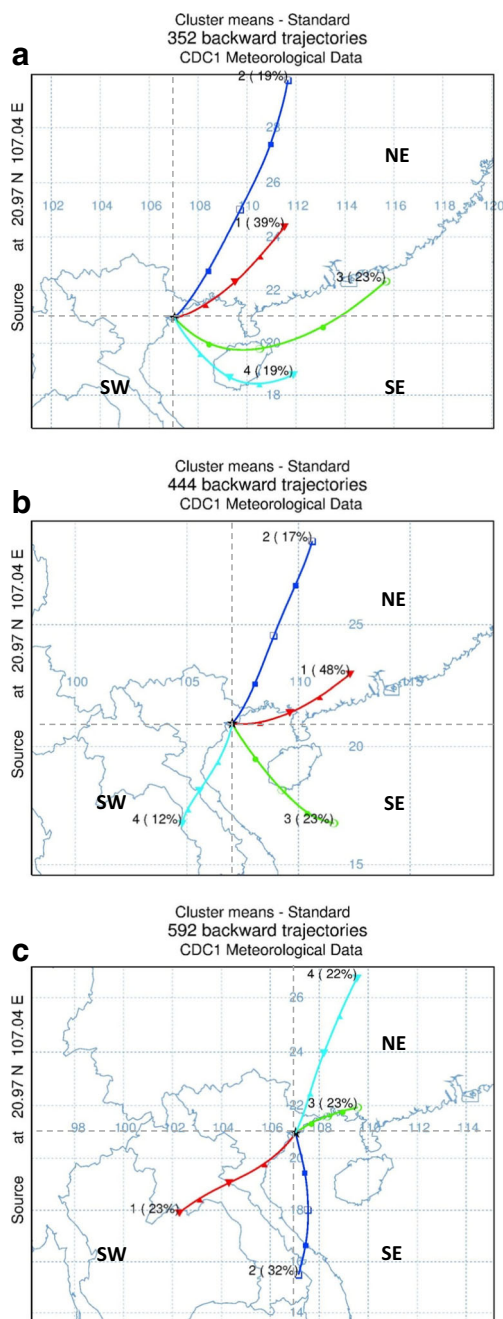


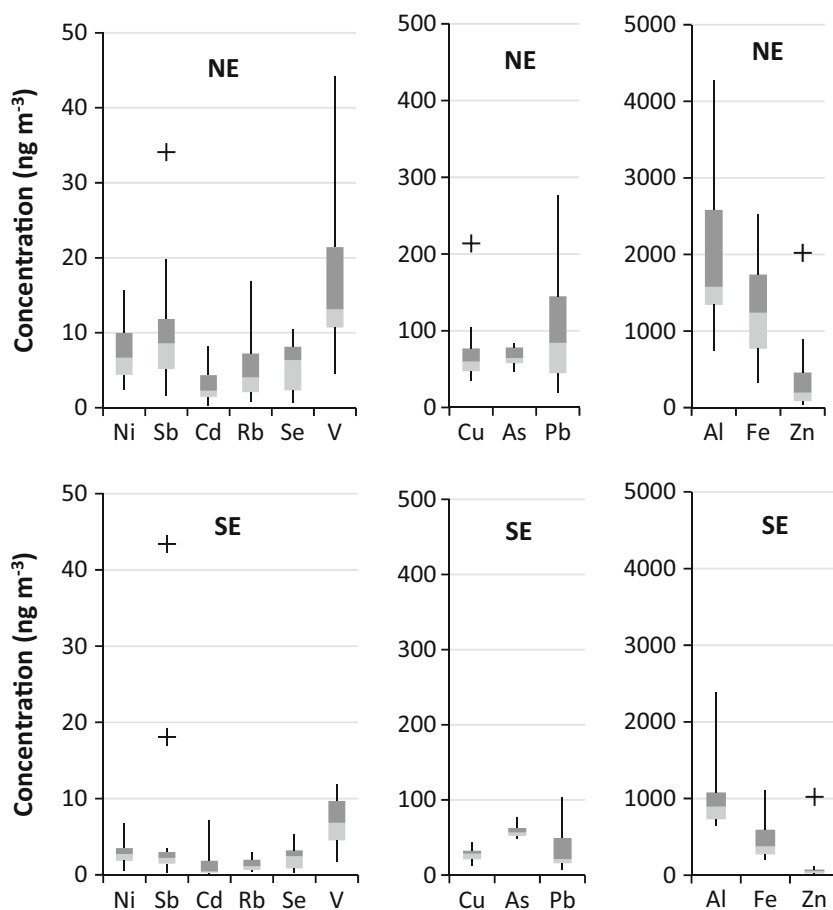
Fig. 1 Statistical cluster analysis of air mass backward trajectories showing the path of air parcels prior to arrival at Haiphong during a wet, b transitional, and c dry periods. Trajectories were calculated using the hybrid single-particle Lagrangian trajectory (HYSPLIT 4) model (NOAA Air Resources Laboratory; www.arl.noaa.gov/ready/hysplit4.html) with meteorological data collected from October 2012 to October 2013

Fig. 2, and concentrations are detailed in Table S3 as supplementary information. PM_{10} metal concentrations showed significant variations from day to day, with a maximum in January and a minimum in July. As expected, higher PM_{10} metal concentrations were observed during the NE monsoon,

and lower metal concentrations were measured in south-easterly wind conditions. With a NE dominant airflow pathway, high PM_{10} levels in Haiphong could be linked to the stable atmospheric conditions, which often originated in China (Cohen et al., 2010b; Hai and Kim Oanh, 2013). The anti-cyclonic conditions implied a higher potential of long-range dust transport in the upper cold air mass, and the subsidence temperature inversion in the near ground layer favoured the accumulation of aerosols (Hien et al., 2002). These particular weather conditions allowed both a regional and a local accumulation of particles, considerably worsening atmospheric pollution in Haiphong. During the SE monsoon, a high-pressure system moves toward the north of the southern hemisphere. The weather in northern Vietnam is governed by moist air masses coming from the Indian Ocean and the South China Sea. Aerosol composition stems from two sources: both from the sea itself in the form of spray from the bursting of bubbles and from the land surface in the form of dust from natural erosion and anthropogenic activities. Therefore, atmospheric trace metal concentrations should be lower during this period due to air mass dilution and washout removal by rainfalls.

To evaluate air pollution levels, the World Health Organization (WHO) Air quality guidelines were used as a reference with a focus on As, Cd, Mn, Ni, Pb, and V in PM_{10} (Table 1). Concentrations of As measured in Haiphong were consistently 6- to 12-fold over the WHO guideline, underlining a threat to human health. The concentrations of PM_{10} observed in Haiphong were equivalent to those of Tokyo, where the atmosphere is known to be seriously polluted by toxic heavy metals (Furuta et al., 2005). In comparison with a rural site located in northern Vietnam (i.e. Tam Dao, Vietnam) or with remote islands (Rishiri, Japan; Jeju, Korea), PM_{10} concentrations in Haiphong were several times higher (Okuda et al., 2006; Kim et al., 2012; Hoang et al., 2014). All metal concentrations in PM_{10} were about 5–10 times higher than those observed in other regions. In particular, Al was 18 times higher than in Tam Dao; As was up to 55 times higher than in Rishiri and Tokyo; Cd was 12–13 times higher than in the remote islands (Rishiri and Jeju); Cu was 26 and 41 times higher than in Tam Dao and Jeju, respectively; Sb was 18 times higher than in Rishiri; Se was 5 and 10 times higher than in Tokyo and Rishiri, respectively; and Zn was up to 28 times higher than in Tam Dao and Rishiri, making these elements good tracers of anthropogenic activities in Haiphong. Conversely, PM_{10} metallic levels were approximately 5-fold lower than concentrations measured in Beijing and 5 to 20 times lower than in Delhi (Okuda et al., 2008; Kumar et al., 2016), two mega-cities known to rank amongst the most polluted cities in the world (WHO, 2016). These findings indicate that atmospheric particles in Haiphong are heavily impacted by trace metal concentrations and may thus have repercussions on human health.

Fig. 2 Box and whisker plots of elemental PM₁₀ levels according to dominant airflow pathway (NE for northeast and SE for southeast) during seasonal sampling from October 2012 to October 2013. The boundary between light and dark grey boxes indicates the median; the light and dark grey boxes indicate the 25th and 75th percentile, respectively; whiskers mark the highest and lowest values of the results. Outliers are represented by “+” symbol. Variations of elements during the study are detailed in Tables 1 and S3



Enrichment factors

The concept of enrichment factor (EF) was developed in the seventies (Chester and Stoner, 1973) to evaluate the anthropogenic contribution of a metal (*x*) above an uncontaminated background level, which was in the same matrix as the examined sample. EF is calculated as:

$$EF_x = \frac{(C_x/C_{ref})_{PM_{10}}}{(C_x/C_{ref})_{background}}$$

where *C_x* is the metal concentration and *C_{ref}* is the concentration of a reference element in PM₁₀ and the background matrix, respectively. Since soil dust contributes to atmospheric PM₁₀, the upper continental crust is usually chosen as background matrix (Chester et al., 1991; Okuda et al., 2008). Concentrations of metals in the upper continental crust were reported in Reimann and Caritat (1998). However, absolute EF values must be used cautiously because there is no consensus on the average elemental composition and literature data vary by several orders of magnitude. Furthermore, the choice of the reference element can also affect the absolute

value of EF. The reference element should be chosen free from contamination, stable, and reflecting geogenic sources. Although several lithogenic elements (Al, Fe, Li, Cs, Rh, etc.) can be used as reference element to estimate EF, Al is the most commonly used due to its high concentration in the lithosphere (Grousset et al., 1995; Reimann and Caritat, 2000; Bergamaschi et al., 2004). Nevertheless, anthropogenic inputs of Al from aluminium smelters, cement plants, and other industrial activities could bias EF values. Contrary to Al, Rb has a very low concentration in the lithosphere and is generally not impacted by anthropogenic activities (Reimann and Caritat, 1998). Despite these theoretical considerations that have been the subject of much discussion (Reimann and Caritat, 1998; 2000; 2005), EFs are commonly used to assess the current level of environmental contamination. EF index includes three classes which ranges depend on the atmospheric PM size. For PM₁₀ (coarse particles from natural and anthropogenic sources), EF < 10 is considered to be a crustal origin, 10 < EF < 500 comes from mixed sources (natural and anthropogenic), and EF > 500 indicates a highly enriched element (Wang et al., 2006a, b; Shelley et al., 2015). For PM_{2.5} (fine particles mainly from anthropogenic sources), EF < 1 is considered to be crustal origin, 1 < EF < 5 shows

Table 1 Geometric mean and min-max metal concentrations in PM₁₀ (ng m⁻³) measured in Haiphong during the study, compared with values (average ± σ; ng m⁻³) in different sites and the WHO air quality guideline in Asia

Site region	Haiphong ^a			Tamdao ^b	Beijing ^c	Tokyo ^d	Rishiri ^e	Jeju ^f	New Delhi ^g	WHO
	Vietnam			Vietnam	Chine	Japan	Japan	Korea	India	
	Mean	Min	Max							
Al	1543	647	5232	100 ± 100	3968 ± 3350	1355 ± 492	251 ± 371	683.9	N/A	N/A
As	63.7	41.5	120	N/A	58.3 ± 60.0	2.14 ± 0.32	1.20 ± 2.10	N/A	31.0	6.6
Cd	1.46	0.135	9.01	1 ± 0	9.02 ± 10.3	2.18 ± 0.28	0.19 ± 0.33	0.2	24.5	5
Co	0.900	0.448	1.90	1 ± 0	5.28 ± 5.37	0.69 ± 0.06	0.18 ± 0.25	1.7	N/A	N/A
Cr	7.82	0.921	35.2	30 ± 10	22.7 ± 19.3	10.9 ± 0.31	2.0 ± 2.2	10.7	170	N/A
Cu	48.2	12.3	214	2 ± 1	146 ± 149	73.7 ± 4.52	7.40 ± 10.2	1.3	294	N/A
Fe	828	205	2524	400 ± 200	6200 ± 4714	1392 ± 180	356 ± 645	471	17,380	N/A
Hg	0.065	0.007	0.831	N/A	N/A	N/A	N/A	N/A	N/A	1000
K	978	315	4506	N/A	N/A	N/A	N/A	198.4	N/A	N/A
Mg	433	203	885	100 ± 100	N/A	N/A	N/A	200.9	N/A	N/A
Mn	44.6	6.65	278	10 ± 20	293 ± 224	43.0 ± 5.51	8.60 ± 12.0	9	N/A	150
Na	923	217	5044	N/A	N/A	576 ± 14.8	N/A	252.4	N/A	N/A
Nd	0.363	0.041	1.992	N/A	N/A	N/A	N/A	N/A	N/A	N/A
Ni	4.69	0.478	15.6	5 ± 0	21.6 ± 21.0	4.64 ± 1.29	1.90 ± 3.40	4.4	42.3	25
Pb	56.0	6.83	349	10 ± 10	570 ± 638	N/A	16 ± 30	8.9	1926	500
Rb	2.64	0.445	16.9	N/A	N/A	1.46 ± 0.26	N/A	N/A	N/A	N/A
Sb	5.52	0.321	43.4	N/A	40.1 ± 42.5	20.1 ± 1.47	0.46 ± 0.62	N/A	73.5	N/A
Se	3.37	0.225	23.5	N/A	12.9 ± 13.8	0.93 ± 0.14	0.49 ± 0.65	N/A	9.00	N/A
Sr	6.43	2.05	48.9	1 ± 0	N/A	N/A	N/A	2.6	145	N/A
Ti	13.0	3.30	36.5	20 ± 10	408 ± 320	140 ± 22.4	27 ± 38	23.7	N/A	N/A
V	10.6	1.63	44.2	6 ± 0	14.1 ± 11.4	6.20 ± 0.55	1.30 ± 1.60	6.6	55.3	1000
Zn	145	14.3	2021	30 ± 20	996 ± 913	271 ± 40.3	16 ± 20	10.3	1843	N/A

N/A not available

^aThis study

^bHoang et al. (2014)

^cOkuda et al. (2008)

^dMizohata et al. (2000)

^eOkuda et al. (2006)

^fKim et al. (2012)

^gKumar et al. (2016)

other inputs beside crustal source, and EF > 5 suggests pre-dominant anthropogenic emissions (Yin et al., 2012).

In this study, EFs were calculated as a first indication of the relative sources, using Al as the reference element. In order to produce reliable information concerning pollution trends, we also used Rb as a reference element and compared EF values with Al normalisation (Fig. 3). Rb or Al normalisation presented similar patterns during the NE and SE airflow pathways. Low EF values (< 10) were found for Al, Co, Fe, K, Mg, Mn, Na, Nd, Rb, Sr, and Ti. These metals showed natural origins due to the long-range transport from desert or marine inputs (Duce et al., 1980; Okuda et al., 2006; Kim et al., 2012; Hoang et al., 2014). Some

elements (i.e. Cr, Cu, Hg, Ni, Pb, V, and Zn) showed EFs between 10 and 500, suggesting anthropogenic contamination from urban and industrial activities (Nriagu and Pacyna, 1988; Sun et al., 2004; Furuta et al., 2005). Only Se, As, Cd, and Sb were highly enriched (EF >> 500), indicating major contaminations from the combustion of fossil fuels in power plants, heating plants, and individual heating facilities (Wang et al., 1999; Tian et al., 2010). Mosher and Duce (1987) estimated that 50% of worldwide anthropogenic Se emissions originated from coal combustion. In addition, Se is often found associated with As, Cd, and Sb in coal combustion (Zeng et al., 2001; Li et al., 2014). EF was a first approach used to identify natural

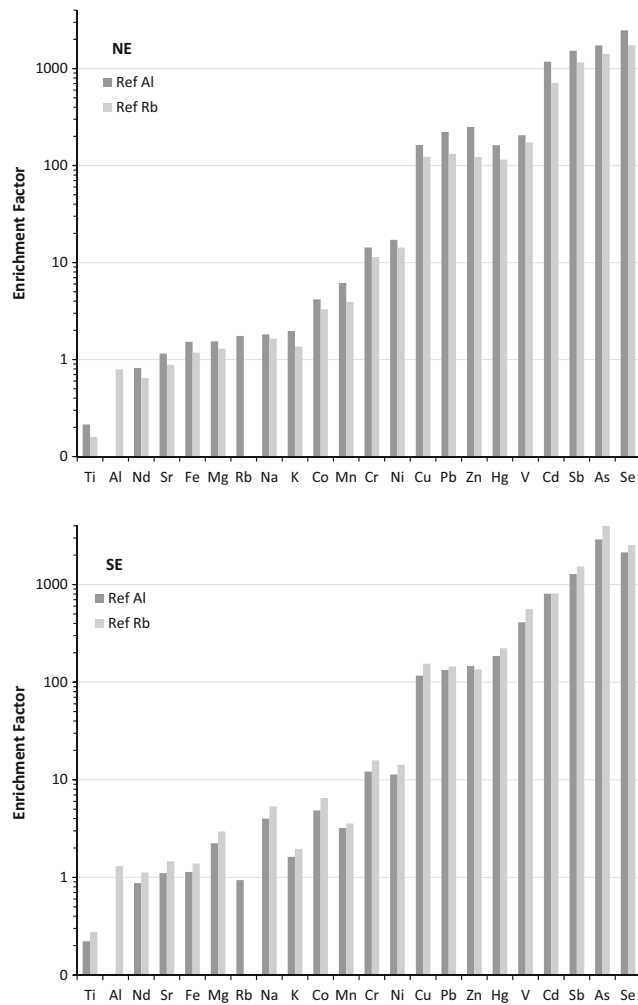


Fig. 3 Average enrichment factors with respect to Al and Rb content (dark and light grey, respectively) in PM₁₀ samples according to air dominant trajectories (NE for northeast and SE for southeast) in Haiphong between October 2012 and October 2013

versus anthropogenic sources in the atmosphere, and Al or Rb were used as reference elements at the sampling site.

Characterisation of anthropogenic emissions

Atmospheric PM is composed of a mixture of elements, which come from different origins. To better assess the emission sources, elemental ratios are often used as markers of PM. However, ratios used in the literature can vary by a factor of 2 to 10 (Nriagu and Pacyna, 1988). Basically, ratios depend on the initial concentration of the trace metals in the raw material and on the primary energy sources used in industrial activities. Atmospheric concentrations of Al and Fe are good indicators of desert dusts (Duce et al., 1975; Kowalczyk et al., 1978) or coal emissions (Gao and Anderson, 2001). In this study, Fe/Al ratios showed variations between 0.3 and 1.5, which is very similar to values obtained from crustal soil (i.e. 0.4) and coal (i.e. 1.1) (Table 2). If natural and anthropogenic inputs have similar chemical balances, the differentiation between sources cannot be clearly established. Nevertheless, our results indicate that Fe/Al ratios were highly correlated with south-easterly wind conditions (mean 0.47 ± 0.17), indicating a typical crustal source (Fig. 4a). Higher concentrations of Fe and Al were observed during the NE airflow pathway. The scattering of elemental ratios up to 1.5 suggested a second source with the possible influence of coal activities during the long-range transport.

Oil combustion is another potential source of metals in PM₁₀. V and Ni have been considered as specific metals from oil combustion in residential, commercial, and industrial applications (Kowalczyk et al., 1978; Pacyna and Pacyna, 2001, Okuda et al., 2007). Traffic is a major source of ground air pollution, especially in urban areas. In Haiphong, with a

Table 2 Selected elemental ratios in natural or anthropogenic sources

Date	Cu/ Sb	Zn/ Pb	Pb/ Cd	Sb/ Cd	Fe/ Al	V/Ni	
Soil							
Chinese soil	19	2.9	260	12	0.44	3.1	Pan et al. (2013)
Crustal soil	77	3.3	185	2.6	0.4	2.9	Reimann and Caritat (1998)
Coal							
Vietnamese coal ^a	9.8	0.7	269	30	N/A	0.55	This study
Chinese coal	22	2.7	50	2.7	1.1	2.6	Pan et al. (2013)
Pretroleum fuels							
Gasoil ^b	3.1	3869	156	114	N/A	0.15	This study
Diesel	10	32	81	44	N/A	0.09	This study
Traffic	6.2	1.7	N/A	5	N/A	1.49–2.4 ^c	Thorpe and Harrison (2008)
Industrial activities							
Steel production	20	0.73	46	0.11	N/A	N/A	Pacyna and Pacyna (2001)
Steel production	N/A	3.5	34	N/A	N/A	N/A	Oravisjarvi et al. (2003)

N/A not available

^a Coc Sau mine

^b #92 unleaded

^c Lee et al. (2000)

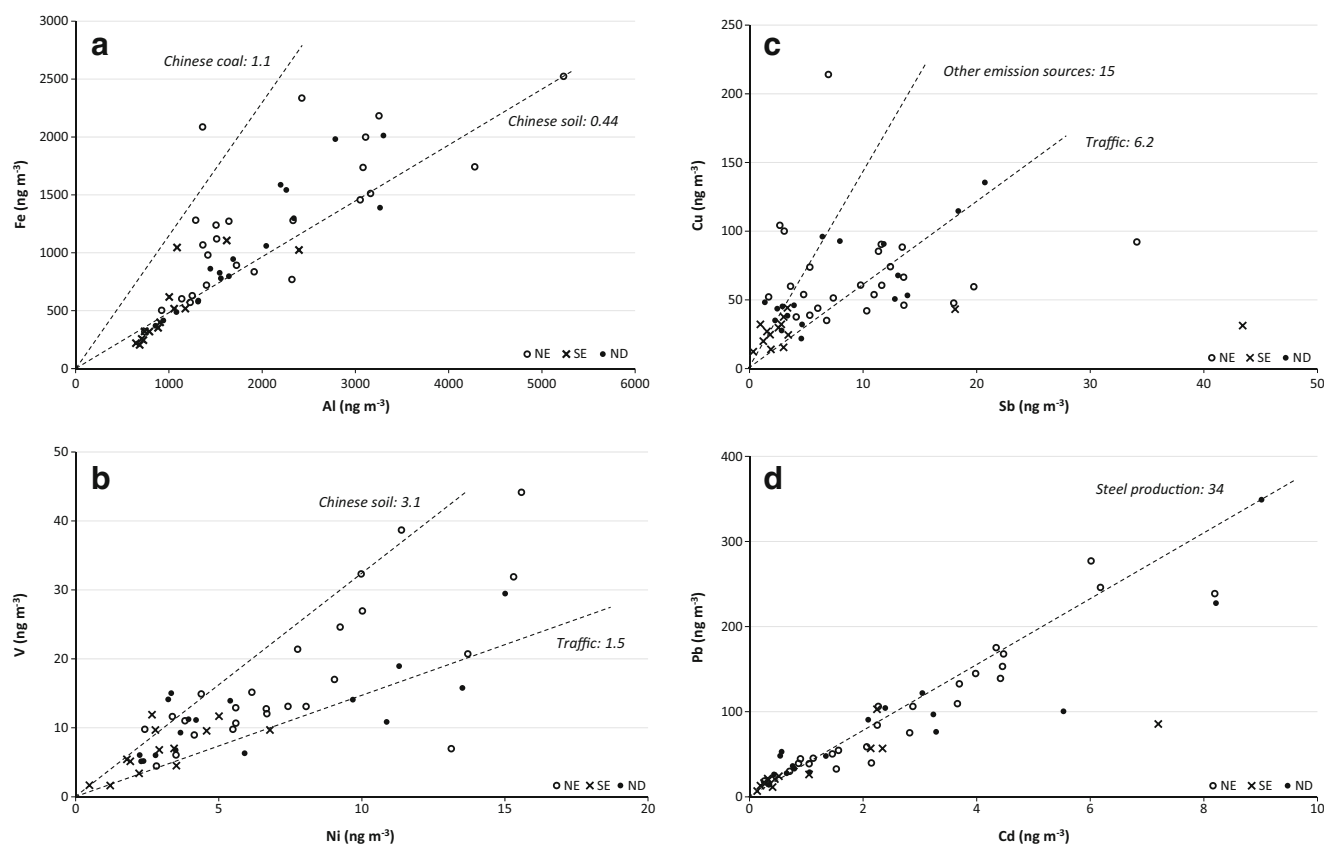


Fig. 4 Chemical balances in PM_{10} collected during sampling periods: **a** Fe vs Al, **b** V vs Ni, **c** Cu vs Sb, **d** Pb vs Cd. Data are presented according dominant air flow pathway using the NOAA HYSPLIT-4 model. Due to the complex back trajectories into transport patterns, we assigned the

dominant wind direction as follow: open circles for northeast (NE), crosses for southeast (SE), and black points for not defined (ND) wind directions. Elemental concentrations are expressed in $ng\ m^{-3}$

population of about two million people and a density of $3600\ people\ km^{-2}$, particles emitted from diesel engines accounted for 25% of the local road resuspension (Vu et al., 2013). In the present study, V/Ni ratios varied between 0.5 and 4.5 with a mean value of 2.4 (Fig. 4b). Elsewhere, a similar range (i.e. 1.49 to 1.9) was obtained in residual oil used in power plants (Swietlicki and Krejci, 1996), and V/Ni values up to 2.4 have been reported by Lee et al. (2000) in oil combustion for domestic heating. The variable ratios between V and Ni mass concentrations in collected samples may result from a spatial and temporal evolution of PM_{10} . Indeed, Sb is commonly used as a flame retardant and is also present in exhaust gas from diesel engine combustion. According to Dietl et al. (1997), road traffic could contribute up to 20% of Sb emissions. Typically, a Cu/Sb ratio of 6 can be imputed to brake lining wear (Thorpe and Harrison, 2008), while higher values (i.e. from 15 to 42) are representative of coal, crustal soil, or steel production (Pacyna and Pacyna, 2001; Zhang et al., 2004; Pan et al., 2013). Within 150 km of Haiphong, there are four coal-fired power stations burning more than 2 million tons of anthracite, three major cement production plants and at least four significant non-ferrous metal factories

(Cohen et al., 2010b). In our samples, these elements presented fingerprints similar to those found in industrial activities of this type (Fig. 4c). Higher Cu/Sb values (between 10 and 30) were not only from crustal soil but also from dust mixed with other anthropogenic emissions. Lower Cu/Sb ratios (between 3 and 10) may be due to dust mixing with fuel oil combustion, as used by road and maritime traffic (respectively, 10 and 3.1, Table 2). The influence of air masses was not clearly established, but the increase of anthropogenic metal concentrations in PM_{10} samples can be explained by the mixing of particles during long-range transport and road dust resuspension. The relative discrepancy of these elements in PM_{10} suggests that much of the ambient pollution, which is not associated with extreme events, is produced locally.

Many other trace metals are emitted from anthropogenic sources. The non-ferrous metal industry accounts for a large fraction of Cd, Cu, Pb (in addition to gasoline combustion), and Zn emitted in the atmosphere. Due to the wide variety of production technologies, it is difficult to select the correct values, but a reasonable range of emission factors can be advanced to highlight this source. Pb/Cd ratios around 40 and Zn/Pb ratios between 0.7 and 3.5

can be used as chemical fingerprints in most non-ferrous emissions (Niagru and Pacyna, 1988; Pacyna and Pacyna, 2001; Oravisjarvi et al., 2003; Sun et al., 2004). Elemental values for the PM₁₀ collected in Haiphong from October 2012 to October 2013 correlated with ratios reported in the literature (Fig. 4d; Fig. S1). The Pb/Cd and Zn/Pb ratios highlighted an enrichment of metallic compounds in atmospheric particles from industrial smelters. As can be seen from the discussion above, the increase of anthropogenic metal concentrations in PM₁₀ samples was made possible via the mixing and the accumulation of particles during long-range transport and road dust resuspension. The study of chemical balances showed that the main anthropogenic sources of PM₁₀ in Haiphong were fossil fuel combustion and industrial activities. Coal combustion was found to be a contributor of Fe and Al in PM₁₀ samples. Oil combustion resulted in the emission of Ni and V into the atmosphere. The non-ferrous metal industry accounted for a fraction of Cu and Zn, with Pb and Sb (in addition to gasoline combustion) also emitted. However, the complex nature of PM₁₀ means that the quantitative estimation of the contribution to each emission source remains difficult and may not be elucidated by chemical element ratios alone.

Lead isotopic source apportionment

Atmospheric emissions are the main cause of metal accumulation in the environment (Nriagu and Pacyna, 1988). The discrimination between these different sources can be assessed by Pb isotopic analysis. In order to estimate the contribution of anthropogenic activities with the greatest accuracy, we used ²⁰⁷Pb/²⁰⁶Pb and ²⁰⁸Pb/²⁰⁶Pb ratios.

Quantification of sources was calculated with a linear mixing model (Monna et al., 1997):

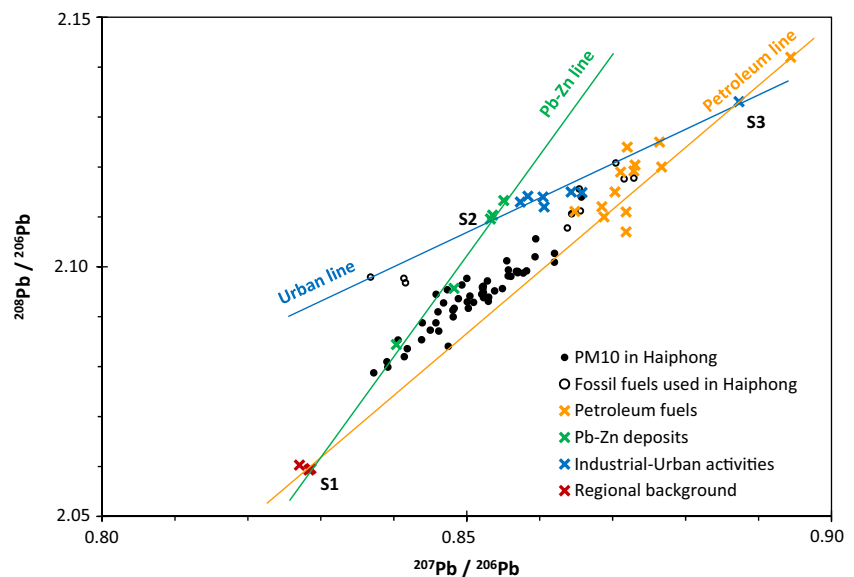
$$\left(\frac{^{207}\text{Pb}}{^{206}\text{Pb}}\right)_m = x_1 \left(\frac{^{207}\text{Pb}}{^{206}\text{Pb}}\right)_1 + x_2 \left(\frac{^{207}\text{Pb}}{^{206}\text{Pb}}\right)_2 + x_3 \left(\frac{^{207}\text{Pb}}{^{206}\text{Pb}}\right)_3$$

$$\left(\frac{^{208}\text{Pb}}{^{206}\text{Pb}}\right)_m = x_1 \left(\frac{^{208}\text{Pb}}{^{206}\text{Pb}}\right)_1 + x_2 \left(\frac{^{208}\text{Pb}}{^{206}\text{Pb}}\right)_2 + x_3 \left(\frac{^{208}\text{Pb}}{^{206}\text{Pb}}\right)_3$$

$$x_1 + x_2 + x_3 = 1$$

where *m* is the measured sample, the numbers in subscript (1, 2, and 3) represent sources, and *x* their relative contribution. Lead isotopic ratios of PM₁₀ collected in Haiphong during our study varied from 0.8373 to 0.8704 for ²⁰⁷Pb/²⁰⁶Pb and from 2.0788 to 2.1208 for ²⁰⁸Pb/²⁰⁶Pb (Fig. 5, Table S4). These ratios were in agreement with recent measurements of Pb isotopic composition in Tay Ho, an urban lake located in the north of Hanoi. Isotopic ratios in the top sediment layer varied from 0.840 to 0.855 for ²⁰⁷Pb/²⁰⁶Pb and from 2.075 to 2.120 for ²⁰⁸Pb/²⁰⁶Pb (Kikuchi et al., 2010). The cities of Hanoi and Haiphong presented a similar isotopic signature, which indicates the same origins of Pb, probably due to atmospheric deposition from long-range dust transport and local resuspension. As discussed earlier, anthropogenic Pb pollution in Haiphong originates mainly from fossil fuel combustion, industrial smelting, and urban activities. The predominant origin

Fig. 5 Relationship between ²⁰⁷Pb/²⁰⁶Pb and ²⁰⁸Pb/²⁰⁶Pb ratios in Haiphong. The black dots are data from PM₁₀ samples and open circles are data from fossil fuels used in Haiphong (Table S4 for description). The coloured data are source values of samples collected in East Asia (see Table 3 for description). The blue line is based on data for urban-industrial activities; the green line corresponds to the Pb isotopic fractionation in Pb-Zn ores, and the orange line corresponds to the Pb isotopic fractionation of petroleum fuels



of Pb in the PM₁₀ collected in Haiphong was further evidenced by plotting Pb isotopic compositions from natural and anthropogenic sources in the same geochemical province.

The majority of countries in the Asia-Pacific region have phased-out leaded gasoline since 2000, with Indonesia being the last of the larger Asian countries to do so in 2006. Other countries, such as Cambodia, Bhutan, Laos, Mongolia, Myanmar, and North Korea, are presumably still using local leaded gasoline, but in quite low amounts (i.e. 2%) comparative to quantities of imported unleaded gasoline (www.acfa.org.sg). Because the isotopic signature of Pb in gasoline has changed substantially due to the discontinuation of alkyl-lead, we limit our comparison to the most recently published references, i.e. those obtained after 2000 (Mukai et al., 2001; Duzgoren-Aydin et al., 2004; Chen et al., 2005; Yao et al., 2015). Lead fingerprints of other anthropogenic activities (mining, smelting, coal combustion, waste incineration, etc.) have been identified by numerous studies (Mukai et al., 1993; Zhu, 1998; Sangster et al., 2000; Bollhofer and Rosman, 2000; Zhu et al., 2001, 2003; Zheng et al., 2004; Chen et al., 2005; Duzgoren-Aydin, 2007; Diaz-Somoano et al., 2009; Zhao et al., 2015). The quantification of anthropogenic inputs also depends on the establishment of natural sources. Haiphong is surrounded by seven geochemical provinces (North China, Northeast China, North Xinjiang, Tibet, Cathaysia, Yangtze, and the Indochinese Peninsula) with different Pb isotopic fingerprints (Zhu et al., 2003; Gallon et al., 2011). Lead isotope composition in natural samples, including basaltic and granitic rocks from the Earth's mantle, shows wide variations. Due to the high heterogeneity in Asian crustal soils, the localization of the natural Pb isotopic background is a complex task. Furthermore, owing to the accelerated population growth and increasing industrial activities in the past decades, it is clear that Pb present in soils comes from a mix of natural and anthropogenic sources. In the Pearl River Delta, no anthropogenic Pb isotopic evidence from continental China could be detected in recent pelagic sediments (Zhu et al., 2003). As sediments in the South China Sea are derived from the lands surrounding the Indochinese Peninsula and the Cathaysian geochemical province in China, the Pb isotopic composition in silty clays was chosen to provide a record of regional background.

The compilation of $^{207}\text{Pb}/^{206}\text{Pb}$ and $^{208}\text{Pb}/^{206}\text{Pb}$ ratios in different Pb origins is detailed in Table 3. We used the less radiogenic ratios ($^{207}\text{Pb}/^{206}\text{Pb} = 0.827$ and $^{208}\text{Pb}/^{206}\text{Pb} = 2.060$) as source S1 to represent the regional background, which reflects the actual combination of natural and anthropogenic background contribution. With the discontinuation of leaded gasoline, the Pb contribution was reduced and the $^{207}\text{Pb}/^{206}\text{Pb}$ increased gradually to approach the Earth growth curve, making this source identification difficult (Cumming and Richards, 1975; Wang et al., 2006a, b). In urban areas, dust resuspension due to road traffic cannot be disregarded. Pb

emissions from industrial or domestic activities may therefore be responsible for a significant portion of Pb atmospheric inputs. In a conventional isotope $^{207}\text{Pb}/^{206}\text{Pb}$ vs $^{208}\text{Pb}/^{206}\text{Pb}$ plot, the mixing between three sources is characterised by a scattering of the sample within a triangle defined by the end members in the bi-dimensional isotope space (Fig. 5). As shown above, coal activity influences Pb levels in PM₁₀. Indeed, the published lead isotope ratios for coal samples from the SE Asian region overlap Haiphong PM₁₀ isotopic ratio ranges (Fig. S2). However, in addition to coal combustion, the Asian region is also known to have numerous Pb-Zn deposits whose lead isotopic composition can be used as a tracer of anthropogenic inputs. Observing the intercept of the “Pb-Zn line” and the “Urban line,” we found that source S2 was located in the closest Chinese province of Cathaysia, in the Fankou Pb-Zn ore deposit ($^{207}\text{Pb}/^{206}\text{Pb} = 0.853$ and $^{208}\text{Pb}/^{206}\text{Pb} = 2.110$). Furthermore, the intercept between the two linear trends, the “petroleum line” and the “urban line,” clearly identified the vehicle exhaust source S3 with Pb isotopic fingerprints ($^{207}\text{Pb}/^{206}\text{Pb} = 0.8873$ and $^{208}\text{Pb}/^{206}\text{Pb} = 2.1331$) obtained from Bangkok, a mega-city with more than 8.2 million automobiles registered in 2013 (Zhu et al., 2003; Narut et al., 2016).

Our Pb isotopic fingerprinting approach clearly demonstrated that PM₁₀ in Haiphong were composed of a mixture of soil dusts and two main anthropogenic inputs from vehicle exhaust and non-ferrous smelters. The contribution of each source was calculated using equations from the linear model (Fig. 6, Table S5). Lead atmospheric inputs were highly influenced by source S1. The average contributions of the regional background varied between 41.5% during the NE airflow pathway and 51.6% with south-easterly wind conditions. These results were easily attributable to Asian dust storms, which transport fine, dry soil particles over vast areas. The increase of the soil dust fraction during the SE monsoon was due to aerosol mixing, with marine airflow less impacted by anthropogenic activities. As discussed above, soil dusts evaluated from source S1 had a combination of natural and anthropogenic inputs. Thus, the contribution of natural dusts from pristine soils may be lower than our estimation (S1), as the overestimation of S1 implies an underestimation of S2 + S3. These considerations show that dominant Pb inputs are from anthropogenic activities. The oil combustion fraction in PM₁₀ samples presented seasonal variations. The average contribution varied between 31.5% during the NE airflow pathway to 20.2% in south-easterly wind conditions. The production of Chinese electricity depends on both industrial demand and outdoor temperature. Firstly, due to low temperatures between October and April, the increase in Chinese energetic demand is supplied via oil combustion (Tian et al., 2012). Secondly, Vietnam's oil consumption is about 450,000 barrels per day, with an expected increase of 10% per year up to 2020 (IEA, 2015). During the NE monsoon, Haiphong received

Table 3 A comparison of Pb isotope composition from different sources in Asia

Location	$^{207}\text{Pb}/^{206}\text{Pb}$	$^{208}\text{Pb}/^{206}\text{Pb}$	$^{206}\text{Pb}/^{204}\text{Pb}$	Sample origin	Reference
Regional soil					
South China Sea	0.828	2.059	18.74	Silty clay	Zhu et al. (2003)
South China Sea	0.827	2.060	19.02	Silty clay	Zhu et al. (2003)
South China Sea	0.829	2.060	19.02	Silty clay	Zhu et al. (2003)
Coal					
Haiphong (Vietnam)	0.8368	2.0979	18.84		This study
Haiphong (Vietnam)	0.8414	2.0977	N/A		This study
Haiphong (Vietnam)	0.8416	2.0968	N/A		This study
Ho Chi Minh (Vietnam)	0.87	2.10	18.01		Bolhofer and Rosman (2000)
Hanoi (Vietnam)	0.86	2.10	18.25		Bolhofer and Rosman (2000)
Indonesia	0.8459	2.0897	N/A		Diaz-Somoano et al. (2009)
Indonesia	0.8472	2.1013	N/A		Diaz-Somoano et al. (2009)
Indonesia	0.8417	2.0878	N/A		Diaz-Somoano et al. (2009)
China	0.8661	2.1249	N/A		Diaz-Somoano et al. (2009)
China	0.849	2.101	N/A		Mukai et al. (1993)
Shanghai (Yangtze Province)	0.8600	2.1111	N/A		Chen et al. (2005)
Dafang (Southern Province)	0.832	2.083	18.75		Zhao et al. (2015)
Guiyang (Southern Province)	0.824	2.060	18.99		Zhao et al. (2015)
Guiyang (Southern Province)	0.804	2.002	19.53		Zhao et al. (2015)
Shanxi (North Province)	0.839	2.071	18.56		Zhao et al. (2015)
Shandong (North Province)	0.837	2.065	18.65		Zhao et al. (2015)
Pb-Zn deposit					
North Province	0.896	2.188	17.23		Zhu et al. (2003)
Cathaysia Province	0.855	2.113	18.42		Zhu et al. (2003)
Indonesia Province	0.840	2.084	18.67		Zhu et al., 2003
Foshan (Cathaysia Province)	0.8535	2.1104	N/A		Zhu (1998)
Fankou (Cathaysia Province)	0.853	2.110	18.35		Sangster et al. (2000)
Jinding (Southern Province)	0.848	2.096	18.45		Sangster et al. (2000)
Petroleum fuels					
Haiphong (Vietnam)	0.8638	2.1078	18.09	Diesel ^a	This study
Haiphong (Vietnam)	0.8654	2.1156	N/A	Diesel ^a	This study
Haiphong (Vietnam)	0.8656	2.1112	N/A	Diesel ^a	This study
Haiphong (Vietnam)	0.8644	2.1106	N/A	#92 gasoline ^a	This study
Haiphong (Vietnam)	0.8729	2.1178	17.86	#92 gasoline ^a	This study
Haiphong (Vietnam)	0.8716	2.1176	N/A	#92 gasoline ^a	This study
Shanghai (Yangtze province)	0.872	2.124	N/A	Traffic	Chen et al. (2005)
Guiyang (Southern Province)	0.8648	2.1111	18.07	Traffic	Zhao et al. (2015)
Hong Kong (Cathaysia Province)	0.8685	2.1120	N/A	Traffic	Duzgoren-Aydin et al. (2004)
Surgut (Russia)	0.88	2.12	17.69	Oil field	Mukai et al. (2001)
Nizhnevartovsk (Russia)	0.89	2.14	17.36	Oil field	Mukai et al. (2001)
Taipei (Taiwan)	0.870	2.115	17.89	Diesel ^b	Yao et al. (2015)
Taipei (Taiwan)	0.872	2.107	17.87	#98 gasoline ^b	Yao et al. (2015)
Taipei (Taiwan)	0.869	2.110	17.94	#95 gasoline ^b	Yao et al. (2015)
Taipei (Taiwan)	0.872	2.111	17.86	#92 gasoline ^b	Yao et al. (2015)
Taipei (Taiwan)	0.871	2.119	17.89	Diesel ^c	Yao et al. (2015)
Taipei (Taiwan)	0.873	2.119	17.85	#98 gasoline ^c	Yao et al. (2015)
Taipei (Taiwan)	0.876	2.125	17.78	#95 gasoline ^c	Yao et al. (2015)
Taipei (Taiwan)	0.873	2.120	17.84	#92 gasoline ^c	Yao et al. (2015)
Industrialised zone					
Bangkok (Thailand)	0.8873	2.1331	17.6	Urban city	Zhu et al. (2003)
Shanghai (Yangtze Province)	0.8606	2.112	18.16	Residencial	Zheng et al. (2004)
Shanghai (Yangtze Province)	0.8643	2.115	18.12	Residencial	Zheng et al. (2004)
Hong Kong (Cathaysia Province)	0.8658	2.1149	N/A	Residencial	Duzgoren-Aydin (2007)
Foshan (Cathaysia Province)	0.860	2.114	N/A	Industrial	Zhu et al. (2001)
Foshan (Cathaysia Province)	0.858	2.114	N/A	Industrial	Zhu et al. (2001)
Foshan (Cathaysia Province)	0.857	2.113	N/A	Industrial	Zhu et al. (2001)

N/A not available

^a Vietnam National Petroleum Group (Petrolimex)

^b Chinese Petroleum Corporation

^c Formosa Plastics Corporation

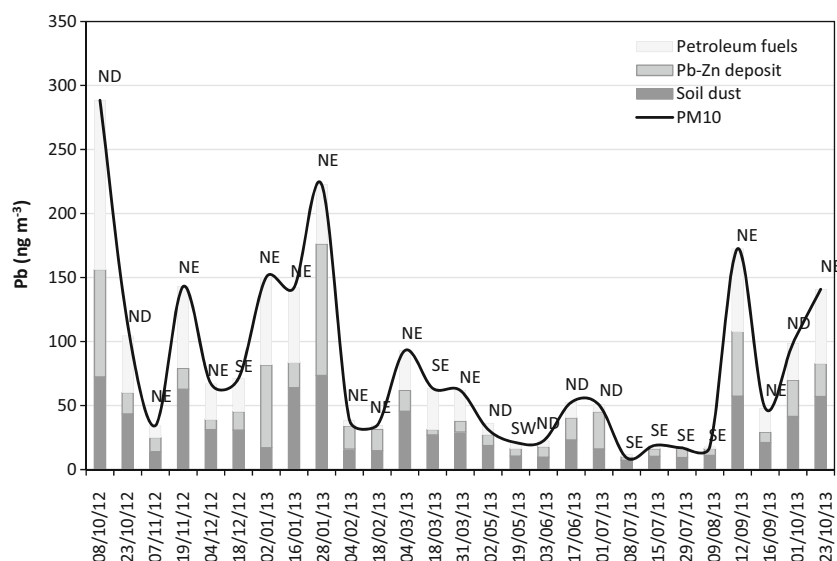


Fig. 6 Variation of Pb content and relative contributions of Pb sources in Haiphong atmospheric particles during the sampling period (October 2012–October 2013). Data are presented according dominant air flow pathway using the NOAA HYSPLIT-4 model. Due to the complex back trajectories into transport patterns, we assigned the dominant wind

direction as follow: open circles for northeast (NE), crosses for southeast (SE), and black points for not defined (ND) wind directions. Elemental concentrations are expressed in ng m^{-3} . The plot figure illustrates the average of two consecutive 12-h sampling periods. For details see Table S5

atmospheric pollution from both the long-range transport of regional dust and from local urban soil resuspension, which increased the contribution of petroleum fuels in PM_{10} samples. In addition to oil combustion, Pb-Zn ore related to industrial emissions also contributed to atmospheric Pb contamination. The average Pb-Zn ore fraction in atmospheric particles varied from 27.0% during the NE airflow pathway to 28.2% during the SE wind events. No seasonal pattern was observed, suggesting a constant Pb-Zn industrial activity over time. In the Pb isotope plot, the Pb-Zn source was clearly located in the Chinese province of Cathaysia, indicating that atmospheric Pb in Haiphong partly results from long-range transport. During the SE monsoon, anthropogenic particles were diluted with marine aerosols. The constant Pb-Zn contribution also suggests a steady contribution from soil dusts.

To determine whether long-range transport or urban soil resuspension drove atmospheric pollution in Haiphong, a binary mixing model was used to attribute a regional-type and a local-type to the Pb- PM_{10} seasonal variations:

$$\text{PM}_{10} = x_r \cdot \text{Regional-type} + x_l \cdot \text{Local-type}$$

$$x_r + x_l = 1$$

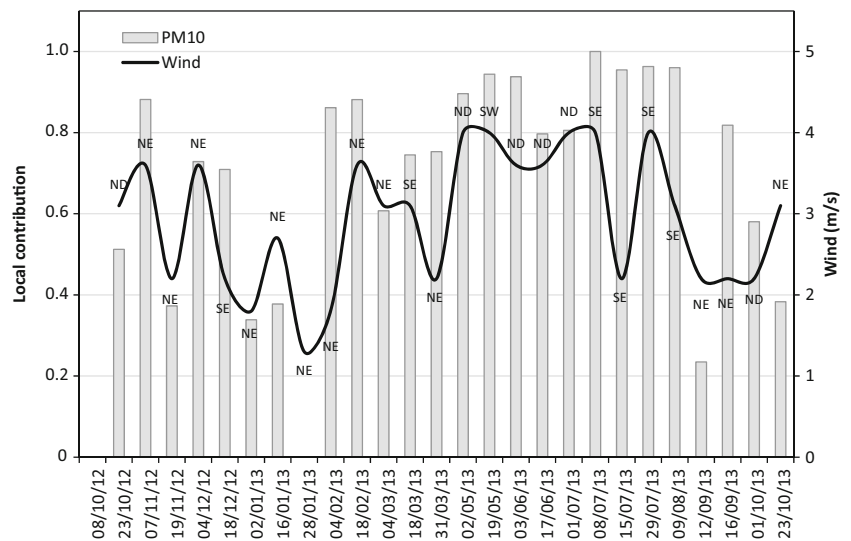
where x_r and x_l represented the contributions of regional and local inputs, respectively. As discussed above, Pb atmospheric concentrations were influenced by both local and regional transport during the NE monsoon. However, rainfalls are known to limit soil dust resuspension by leaching surfaces. In our study, the maximum Pb- PM_{10} level was collected on 28–29 January 2013 during both NE dominant airflow and a rainfall event, suggesting that regionally emitted Pb might be

much more significant than Pb from local inputs. Therefore, the maximum Pb- PM_{10} over 24-h sampling (222.5 ng m^{-3} , 28–29/01/2013) was attributed as regional-type. Conversely, during the SE monsoon, high temperatures favoured air convection and higher wind speed caused the local dispersion of atmospheric particles. In addition, the sub-tropical climate also favoured rainfall, which prevented the resuspension of soil dusts. Local-type was selected during stable SE airflow and a limited rainfall event. These meteorological conditions were recorded on the 08–09 July 2013 with a mean Pb- PM_{10} measured at 9.19 ng m^{-3} over 24-h sampling. As expected, the local- PM_{10} increased with wind speed at the site with a maximal and stable fraction (about 90%) during the SE monsoon and a highly variable fraction with north-easterly wind conditions (Fig. 7, Table S6). Fluctuations with the NE airflow pathway indicated that long-range transport was not negligible. Depending on the regional meteorological event, the regional- PM_{10} fraction could represent from 70 to 100% of atmospheric particles in Haiphong. Our results were in good agreement with a recent study realised in Guiyang (SE China). Indeed, Zhao et al. (2015) have shown that Pb in atmospheric particles was characterised by a decrease in coal combustion and an increase in Pb-Zn industrial emissions, indicating that the locally emitted Pb should be more significant than that from long-range transport.

Conclusion

The combined use of metal measurements with Pb isotopic analysis allowed us to assess contamination levels and

Fig. 7 Variation of contribution of soil dust resuspension as a function of wind speed (m s^{-1}) in Haiphong during the sampling period (October 2012 to October 2013). Data are presented according dominant air flow pathway using the NOAA HYSPLIT-4 model. Due to the complex back trajectories into transport patterns, we assigned the dominant wind direction as follow: open circles for northeast (NE), crosses for southeast (SE), and black points for not defined (ND) wind directions. The plot figure illustrates the average of two consecutive 12-h sampling periods. For details see Table S6



to identify and quantify the sources of PM_{10} in Haiphong. This approach was also used to infer the contribution of specific inputs. High variability of trace metal concentrations was observed in atmospheric particles and revealed a seasonal trend: elevated levels during the NE monsoon and low levels in south-easterly wind conditions. Some elements (As, Cd, Mn) were found in excess of the WHO guidelines, thus posing a potential threat to health and environmental resources. EFs revealed that the composition of PM_{10} collected in Haiphong had various origins. Elements, such as Al, Co, Fe, K, Mg, Mn, Na, Nd, Rb, Sr, and Ti, originated from crustal sources, while other trace metals (Cr, Cu, Hg, Ni, Pb, V, and Zn) were emitted from urban/industrial activities. Coal combustion was highlighted with EFs of As, Cd, Se, and Sb, whose values largely exceeded all others. The study of chemical balances showed that atmospheric pollution in Haiphong was mainly controlled by industrial and/or vehicle exhaust emissions with typical markers of oil combustion such as V/Ni and Cu/Sb ratios (1.5 and 6.2, respectively) and typical markers of industrial activities, such as Pb/Cd and Zn/Pb ratios (34 and 3.5, respectively). The Pb isotope and concentration analyses were used to quantify inputs and to study aerosol transport. PM_{10} showed an important soil dust contribution (constant annual fraction 45% with a relative maximum up to 60% during SE monsoon). Anthropogenic Pb was estimated as the dominant input. Sources were assigned to vehicle exhaust and Pb-Zn smelters as markers of oil combustion and industrial activities, respectively. Whereas oil combustion input was correlated to the dominant airflow pathway (31% during the north-easterly winds and 20% during the south-easterlies), the industrial activity contribution was stable (around 28%) over the year. This distribution can be explained by the transport of local and regional air masses.

During the SE monsoon, anthropogenic Pb was mainly assigned to local soil dust resuspension (about 90%), and during the NE monsoon, the increase of Pb- PM_{10} was due to the mixing of local and regional inputs.

Funding information This work was supported by the French national programme EC2CO-Biohefect/Ecodyn/Dril/Microbien (Project SOOT), the French-Vietnamese Hubert Curien Partnership (contract no. 23971TK), and the Vietnamese Ministry of Science and Technology (contract no. 46/2012/HD-NDT). The project leading to this publication has received funding from European FEDER Fund under project 1166-39417.

References

BGR (Bundesanstalt für Geowissenschaften und Rohstoffe) (2013) Reserves, resources and availability of energy resources. Energy Study Report, Hannover, p 112

Bergamaschi L, Rizzio E, Giaveri G, Profumo A, Loppi S, Gallorini M (2004) Determination of baseline element composition of lichens using samples from high elevations. *Chemosphere* 55:933–939

Bollhofer A, Rosman KJR (2000) Isotopic source signatures for atmospheric lead: the Southern Hemisphere. *Geochim Cosmochim Acta* 64:3251–3262

Chen JM, Tan MG, Li YL, Zhang YM, Lu WW, Tong YP, Zhang GL, Li Y (2005) A lead isotope record of Shanghai atmospheric lead emissions in total suspended particles during the period of phasing out of leaded gasoline. *Atmos Environ* 39:1245–1253

Chen GQ, Zhang B (2010) Greenhouse gas emission in China 2007: inventory and input-output analysis. *Energy Policy* 38:6180–6193

Chester R, Stoner JH (1973) Pb in particulates from the lower atmosphere of the eastern Atlantic. *Nature* 245:27–28

Chester R, Berry AS, Murphy KJT (1991) The distributions of particulate atmospheric trace metals and mineral aerosols over the Indian Ocean. *Mar Chem* 34:261–290

Cohen DD, Crawford J, Stelcer E, Bac VT (2010a) Characterization and source apportionment of fine particulate sources at Hanoi from 2001 to 2008. *Atmos Environ* 44:320–328

- Cohen DD, Crawford J, Stelcer E, Bac VT (2010b) Long range transport of fine particle windblown soils and coal fired power station emissions into Hanoi between 2001 to 2008. *Atmos Environ* 44:3761–3769
- Cumming GL, Richards JR (1975) Ore lead isotope ratios in a continuously changing earth. *Earth Planet Sci Lett* 28:155–171
- Diaz-Somoano M, Kylander E, Lopez-Anton MA, Suarez-Ruiz I, Martinez-Tarazona MR, Ferrat M, Kober B, Weis S (2009) Stable lead isotope compositions in selected coals from around the world and implications for present day aerosol source tracing. *Environ Sci Technol* 43:1078–1085
- Dietl C, Reifenhäuser W, Peichl L (1997) Association of antimony with traffic occurrence in airborne dust, deposition and accumulation in standardized grass culture. *Sci Tot Environ* 205:235–244
- Doe BR (1970) Lead Isotopes. Minerals, Rocks and Inorganic Materials. Monograph Series of Theoretical and Experimental Studies 3. Springer, Berlin, p 143
- Draxler RR, Stunder B, Rolph G, Taylor A (1999) HYSPLIT-4 user's guide. NOAA Technical Memorandum, ERL, ARL 230:1–35
- Draxler RR, Rolph GD (2003) HYSPLIT (Hybrid Single-Particle Lagrangian Integrated Trajectory). Model access via NOAA ARL READY Website (<http://ready.arl.noaa.gov/HYSPLIT.php>). NOAA Air Resources Laboratory, Silver Spring, MD
- Duan FK, Liu XD, He KB, Lu YQ, Wang L (2003) Atmospheric aerosol concentration level and chemical characteristics of water-soluble ionic species in wintertime in Beijing, China. *J Environ Monitor* 5: 569–573
- Duce RA, Hoffman GL, ZoUer WH (1975) Atmospheric trace metals at remote Northern and Southern Hemisphere sites: pollution or natural. *Science* 187:59–61
- Duce RA, Unni CK, Ray BJ, Prospero JM, Merrill JT (1980) Long-range atmospheric transport of soil dust from Asia to the tropical North Pacific: temporal variability. *Science* 209:1522–1524
- Duzgoren-Aydin NS, Li XD, Wong SC (2004) Lead contamination and isotope signatures in the urban environment of Hong Kong. *Environ Int* 30:209–217
- Duzgoren-Aydin NS (2007) Sources and characteristics of lead pollution in the urban environment of Guangzhou. *Sci Tot Environ* 385:182–195
- EPA (1999) Determination of trace metals in ambient particulate matter using inductively coupled plasma mass spectrometry (ICP/MS). Compendium of methods IO-3.5, EPA/625/R-96/010a
- Feng JL, Chan CK, Fang M, Hu M, He LY, Tang XY (2005) Impact of meteorology and energy structure on solvent extractable organic compounds of PM_{2.5} in Beijing, China. *Chemosphere* 61:623–632
- Furuta N, Akihiro I, Akiko K, Kazuhiro S, Keiichi S (2005) Concentrations, enrichment and predominant sources of Sb and other trace elements in size classified airborne particulate matter collected in Tokyo from 1995 to 2004. *J Environ Monit* 7:1155–1161
- Gallon C, Ranville MA, Conaway CH, Landing WL, Buck CS, Morton PL, Flegal AR (2011) Asian industrial lead inputs to the North Pacific evidenced by lead concentrations and isotopic compositions in surface waters and aerosols. *Environ Sci Technol* 45:9874–9882
- Gatari MJ, Boman J, Wagner A, Janhall S, Isakson J (2006) Assessment of inorganic content of PM_{2.5} particles sampled in a rural area north-east of Hanoi, Vietnam. *Sci Total Environ* 368:675–685
- Gao Y, Anderson JR (2001) Characterization of Chinese aerosols determined by individual particle analysis. *J Geophys Res* 106:18037–18045
- Grousset FE, Quétel CR, Thomas B, Donard OFX, Lambert CE, Guillard F, Monaco A (1995) Anthropogenic vs. lithogenic origins of trace elements (As, Cd, Pb, Rb, Sb, Sc, Sn, Zn) in water column particles: northwestern Mediterranean Sea. *Mar Chem* 48:291–310
- Hai CD, Kim Oanh NT (2013) Effects of local, regional meteorology and emission sources on mass and compositions of particulate matter in Hanoi. *Atmos Environ* 78:105–112
- Henry RC, Lewis CW, Hopke PK, Williamson HJ (1984) Review of receptor model fundamentals. *Atmos Environ* 18:1507–1515
- Hien PD, Bihn NT, Truong Y, Ngo NT, Sieu LN (2001) Comparative receptor modelling study of TSP, PM₂ and PM₂₋₁₀ in Ho Chi Minh City. *Atmos Environ* 35:2669–2978
- Hien PD, Bac VT, Tham HC, Nhan DD, Vinh LD (2002) Influence of meteorological conditions on PM_{2.5} and PM₁₀ concentrations during the monsoon season in Hanoi, Vietnam. *Atmos Environ* 36:3473–3484
- Hien PD, Bac VT, Thinh NTH (2004) PMF receptor modelling of fine and coarse PM₁₀ in air masses governing monsoon conditions in Hanoi, northern Vietnam. *Atmos Environ* 38:189–201
- Hoang XC, Nghiem TD, Nguyen TD, Nguyen TKO, Nguyen TH, Nguyen HP, Hoang AL (2014) Levels and composition of ambient particulate matter at a mountainous rural site in Northern Vietnam. *Aerosol Air Qual Res* 14:1917–1928
- Hu CW, Chao MR, Wu K-Y, Chan-Chien GP, Lee WJ, Chang LW, Lee WS (2003) Characterization of multiple airborne particulate metals in the surroundings of a municipal waste incinerator in Taiwan. *Atmos Environ* 37:2845–2852
- IEA (International Energy Agency) (2015) Southeast Asia energy outlook 2015. World Energy Outlook Special Report, OECD/IEA, Paris, p 139
- Kikuchi T, Hai HT, Tanaka S (2010) Characterization of heavy metal contamination from their spatial distribution in sediment of an urban lake of Hanoi, Vietnam. *J Water Environ Technol* 8:111–123
- Kim W, Song JM, Ko HJ, Kim JS, Lee JH, Kang CH (2012) Comparison of chemical compositions of size-segregated atmospheric aerosols between Asian dust and non-Asian dust periods at background area of Korea. *Bull Kor Chem Soc* 33:3651–3656
- Komárek M, Ettler V, Chrastny V, Milhaljevic M (2008) Lead isotopes in environmental sciences: a review. *Environ Int* 34:562–577
- Kowalczyk GS, Choquette CE, Gordon GE (1978) Chemical element balances and identification of air pollution sources in Washington, D.C. *Atmos Environ* 12:1143–1153
- Kumar S, Aggarwal SG, Malherbe J, Barre JPG, Beraill S, Gupta PK, Donard OFX (2016) Tracing dust transport from Middle-East over Delhi in March 2012 using metal and lead isotope composition. *Atmos Environ* 132:179–187
- Lee SW, Pomalis R, Kan B (2000) A new methodology for source characterization of oil combustion particulate matter. *Fuel Process Technol* 65-66:189–202
- Li H, Liu G, Cao Y (2014) Content and distribution of trace elements and polycyclic aromatic hydrocarbons in fly ash from a coal-fired CHP plant. *Aerosol Air Quality Res* 14:1179–1188
- Manhès G, Minster JF, Allègre CJ (1978) Comparative U-Th-Pb and Rb-Sr study of the St. Severin amphoterite: consequence for early solar system chronology. *Earth Planet Sci Lett* 39:14–24
- Monna F, Lancelot J, Croudace IW, Cundy AB, Lewis JT (1997) Pb isotopic composition of airborne particulate material from France and the southern United Kingdom: implications for Pb pollution sources in urban areas. *Environ Sci Technol* 31:2277–2286
- Mosher BW, Duce RAA (1987) A global atmospheric selenium budget. *J Geophys Res* 98:16777–16788
- Mukai H, Tanaka A, Fujii T (1991) Lead isotope ratios of airborne particulate matter as tracers of long-range transport of air pollutants around Japan. *J Geophys Res* 99:3717–3726
- Mukai H, Furuta N, Fujii T, Amb Y, Sakamoto K, Hashimoto Y (1993) Characterization of sources of lead in the urban air of Asia using ratios of stable lead isotopes. *Environ Sci Technol* 27:1347–1356
- Mukai H, Tanaka A, Fujii T, Zeng Y, Hong Y, Tang J, Guo S, Xue H, Sun Z, Zhou J, Xue D, Zhao J, Zhai G, Gu J, Zhai P (2001) Regional characteristics of sulphur and lead isotope ratios in the atmosphere at several Chinese urban sites. *Environ Sci Technol* 35:1064–1071

- Murozumi M, Chow TJ, Patterson CC (1969) Chemical concentrations of pollutant lead aerosols, terrestrial dusts and sea salts in Greenland and Antarctic snow strata. *Geochim Acta* 33:1247–1294
- Narut S, Kraichat T, Tassanee P (2016) Ambient PM₁₀ and PM_{2.5} concentrations at different high traffic-related street configurations in Bangkok, Thailand. *Southeast J. Trop. Med. Public Health* 47: 528–535
- Nriagu JO, Pacyna JM (1988) Quantitative assessment of worldwide contamination of air, water and soils by trace metals. *Nature* 333: 134–139
- Okuda T, Tenmoku M, Kato J, Mori J, Taishi S, Yokochi R, Tanak S (2006) Long term observation of trace metal concentration in aerosols at a remote island, Rishiri, Japan by using inductively coupled plasma mass spectrometry equipped with laser ablation. *Water Air Soil Pollut* 174:3–17
- Okuda T, Nakao S, Katsuno M, Tanaka S (2007) Source identification of nickel in TSP and PM_{2.5} in Tokyo, Japan. *Atmos Environ* 41:7642–7648
- Okuda T, Katsuno M, Naoi D, Nakao S, Tanaka S, He K, Ma Y, Lei Y, Jia Y (2008) Trends in hazardous trace metal concentrations in aerosols collected in Beijing, China from 2001 to 2006. *Chemos* 72:917–924
- Oravitsjarvi K, Timonen KL, Wiikinkoski T, Ruuskanen AR, Heinanen K, Ruuskanen J (2003) Source contributions to PM_{2.5} particles in the urban air of a town situated close to a steel works. *Atmos Environ* 37:1013–1022
- Ortega GS, Pécheyran C, Bérail S, Donard OF (2012) A fit-for purpose procedure for lead isotopic ratio determination in crude oil, asphaltene and kerogen samples by MC-ICP-MS. *J Anal At Spectrom* 27:1447–1456
- Paatero P, Tapper U (1994) Positive matrix factorisation: a non-negative factor model with optimal utilisation of error estimates of data values. *Environmetrics* 5:111–126
- Pacyna JM, Pacyna EG (2001) An assessment of global and regional emissions of trace metals to the atmosphere from anthropogenic sources worldwide. *Environ Rev* 9:269–298
- Pan Y, Wang Y, Sun Y, Tian S, Cheng M (2013) Size-resolved aerosol trace elements at a rural mountainous site in Northern China: importance of regional transport. *Sci Tot Environ* 461–462:761–771
- Patterson CC, Settle DM (1987) Review of data on eolian fluxes of industrial and natural lead to the lands and seas in remote regions on a global scale. *Mar Chem* 22:137–162
- Pekney NJ, Davidson CL (2005) Determination of trace elements in ambient aerosol samples. *Anal Chim Acta* 540:269–277
- Ramanathan V, Chung C, Kim D, Bettge T, Buja L, Kiehl JT, Washington WM, Fu Q, Sikka DR, Wild M (2005) Atmospheric brown clouds: impacts on South Asian climate and hydrological cycles. *PNAS* 102:5326–5333
- Reimann C, de Caritat P (1998) *Chemical elements in environment*. Springer-Verlag, Berlin, p 398
- Reimann C, de Caritat P (2000) Intrinsic flaws of element enrichment factors (EFs) in environmental geochemistry. *Environ Sci Technol* 34:5084–5091
- Reimann C, de Caritat P (2005) Distinguishing between natural anthropogenic sources for elements in the environment: regional geochemical surveys versus enrichment factors. *Sci Tot Environ* 337:91–107
- Rückerl R, Schneider A, Breitner S, Cyrus J, Peters A (2011) Health effects of particulate air pollution: a review of epidemiological evidence. *Inhal Toxicol* 23:555–592
- Sangster DF, Outridge PM, Davis WJ (2000) Stable lead isotope characteristics of lead ore deposits of environmental significance. *Environ Rev* 8:115–147
- Shelley R, Morton PL, Landing WM (2015) Elemental ratios and enrichment factors in aerosols from the US-GEOTRACES North Atlantic transects. *Deep-Sea Res* 116:262–272
- Stacey JS, Kramers JD (1975) Approximation of terrestrial lead isotope evolution by a two-stage model. *Earth Planet Sci Lett* 26:207–221
- Sun Y, Zhuang G, Wang Y, Han L, Guo J, Dan M, Zhang W, Wang Z, Hao Z (2004) The air-borne particulate pollution in Beijing—concentration, composition, distribution and sources. *Atmos Environ* 38:5991–6004
- Swietlicki E, Krejci R (1996) Source characterization of the Central European atmospheric aerosol using multivariate statistical methods. *Nucl Instrum Methods Phys Res Sect B* 109/110:519–525
- Tian HZ, Wang Y, Xue ZG, Cheng K, Qu YP, Chai FH, Hao JM (2010) Trend and characteristics of atmospheric emissions of Hg, As and Se from coal combustion in China, 1980–2007. *Atmos Chem Phys* 10: 11905–11919
- Tian H, Cheng K, Wang Y, Zhao D, Lu L, Jia W, Hao J (2012) Temporal and spatial variation characteristics of atmospheric emissions of Cd, Cr and Pb from coal in China. *Atmos Environ* 50:157–163
- Thorpe A, Harrison RM (2008) Sources and properties of non-exhaust particulate matter from road traffic: a review. *Sci Tot Environ* 400: 270–282
- Veron A, Church TM, Patterson CC, Erel Y, Merrill JT (1992) Continental origin and industrial sources of trace metals in the Northwest Atlantic troposphere. *J Atm Chem* 14:339–351
- Vu TT (1994) *Estuarine ecosystems of Vietnam*. Science and Technics Publishing House, Hanoi, Vietnam
- Vu VH, Le XQ, Pham NH, Hens L (2013) Application of GIS and modeling in health risk assessment for urban road mobility. *Environ Sci Pollut Res* 20:5138–5149
- Wang CF, Chang CY, Chin CJ, Men LC (1999) Determination of arsenic and vanadium in airborne related reference materials by inductively coupled plasma-mass spectrometry. *Anal Chim Acta* 392:299–306
- Wang X, Bi X, Sheng G, Fu J (2006a) Chemical composition and sources of PM₁₀ and PM_{2.5} aerosols in Guangzhou, China. *Environ Monit Assess* 119:425–439
- Wang J, Guo P, Li X, Zhu J, Reinert T, Heitmann J, Spemann D, Vogt J, Flammeyer RH, Butz T (2000) Source identification of lead pollution in the atmosphere of Shanghai city by analyzing single aerosol particles (SAP). *Environ Sci Technol* 34:1900–1905
- Wang Y, Zhuang G, Sun Y, An Z (2005) Water-soluble part of the aerosol in the dust storm season—evidence of the mixing between mineral and pollution aerosols. *Atmos Environ* 39:7020–7029
- Wang Y, Zhuang G, Sun Y, An ZS (2006b) The variation of characteristics and formation mechanisms of aerosols in dust, haze, and clear days in Beijing. *Atmos Environ* 40:6579–6591
- Wedepohl KH (1995) The composition of the continental crust. *Geochim Cosmochim Acta* 59:217–1232
- WHO (2016) WHO's ambient (outdoor) air pollution database, by country and city. WHO, Geneva http://www.who.int/phe/health_topics/outdoorair/databases/cities/en/
- Wiśniewska K, Lewandowska AU, Witkowska A (2017) Factors determining dry deposition of total mercury and organic carbon in house dust of residents of the Tri-city and the surrounding area (Baltic Sea coast). *Air Qual Atmos Health* 10:821–832
- Yao PH, Shyu GS, Chang YF, Chou YC, Shen CC, Chou CS, Chang TK (2015) Lead isotope characterization of petroleum fuels in Taipei, Taiwan. *Int J Environ Res Public Health* 12:4602–4616
- Yin L, Niu Z, Chen X, Chen J, Xu L, Zhang F (2012) Chemical composition of PM_{2.5} aerosol during haze periods in the mountainous city of Yong'an, China. *J Env Sci* 24:1225–1233
- Zeng T, Sarofim AF, Senior C (2001) Vaporisation of arsenic, selenium and antimony during coal combustion. *Combust Flame* 126:1714–1724
- Zhang J, Ren D, Zhu Y, Chou CL, Zeng R, Zheng B (2004) Mineral matter and potentially hazardous trace elements in coals from Qianxi Fault Depression Area in southwestern Guizhou, China. *Int J Coal Geol* 57:49–61
- Zhao ZQ, Zhang W, Li XD, Yang Z, Zheng HY, Ding H, Wang QL, Xiao J, Fu PQ (2015) Atmospheric lead in urban Guiyang, Southwest China: isotopic source signatures. *Atmos Environ* 115:163–169

- Zheng J, Tan M, Yasuyuki S, Atsushi T, Li Y, Zhang G, Zhang Y, Shan Z (2004) Characteristics of lead isotope ratios and elemental concentrations in PM₁₀ fraction of airborne particulate matter in Shanghai after the phase-out lead gasoline. *Atmos Environ* 38:1191–1200
- Zhu B (1998) The mapping of geochemical provinces in China based on Pb isotopes. *J Geochem Explor* 55:171–181
- Zhu BQ, Chen YW, Peng JH (2001) Lead isotope geochemistry of the urban environment in the Pearl River Delta. *Appl Geochem* 16:409–417
- Zhu BQ, Chen YW, Chang XY (2003) Application of Pb isotopic mapping to environmental evaluation in China. *Chem Speciat Bioavailab* 14:49–56